1 D Calculations on Transport, Neutral Injection Heating and Ignition Control in ZEPHYR

O. Gruber

IPP 1/177 December 1979

MAX-PLANCK-INSTITUT FÜR PLASMAPHYSIK

8046 GARCHING BEI MÜNCHEN

MAX-PLANCK-INSTITUT FÜR PLASMAPHYSIK

GARCHING BEI MÜNCHEN

1 D Calculations on Transport, Neutral Injection Heating and Ignition Control in ZEPHYR

O. Gruber

IPP 1/177 December 1979

Die nachstehende Arbeit wurde im Rahmen des Vertrages zwischen dem Max-Planck-Institut für Plasmaphysik und der Europäischen Atomgemeinschaft über die Zusammenarbeit auf dem Gebiete der Plasmaphysik durchgeführt.

IPP 1/177 O. Gruber

1 D Calculations on Transport, Neutral Injection Heating and Ignition Control in ZEPHYR

December 1979
(in English)

Abstract

1 - d transport calculations and particle trajectory calculations for neutral injection in Zephyr show that without impurity radiation losses a heating power of 20 MW and a pulse length of 1 s should be sufficient to reach ignition in Zephyr (average densities in the compressed stage between 2 and 4.5×10^{14} cm^{-3}). The injection system should have an acceleration voltage of 160 keV; lower energy neutrals require higher heating powers. Heating of the plasma in the compressed stage requires neutral particle energies of $\gtrsim$ 250 keV. Active burn control of the nearly ignited plasma is possible with heating powers of about 1 MW and response times of the feedback system smaller than 200 ms.

1D Calculations on Transport, Neutral Injection Heating and Ignition Control in Zephyr

O. Gruber

In order to go beyond simple scaling laws and determine the ignition conditions and the necessary neutral particle heating in Zephyr /1,2/, transport calculations were made with the 1D Whist code /3/, and particle trajectory calculations with the Freya code /4/. In addition, the stabilization at the lower ignition point by means of neutral injection after adiabatic compression was investigated.

1. 1D Whist Code

Besides including classical losses, the Whist II code takes the following effects into account as well: radiation, Ware pinch, refuelling or gas puffing, anomalous electron losses with a diffusion coefficient adapted to the Alcator results ($\chi_e\,[cm^2\,s^{-1}] = 6.25 \cdot 10^{17} / n_e\,[cm^{-3}]$), enhanced ion losses with an enhancement factor preceding the neo-classical ion heat conduction, ohmic heating, alpha particle heating and neutral injection with variable injection angle, beam energy and beam cross-section. Here the fast ions immediately transfer their energy to the background plasma. The adiabatic compression is described by a subroutine which, in accordance with the adiabatic scaling laws, transforms the n_e, T_e and T_i profiles resulting from the neutral injection phase and uses them as input for simulating the compressed plasma. Losses during the compression phase are ignored here since they are partially compensated by continual neutral particle heating and energy increase of the circulating hot deuterons and α particles by the compression process itself. This line of argument is confirmed by the first calculations with the Baldur code (K. Lackner, R. Wunderlich), in which the adiabatic compression is treated as resolved in time. For the time being the calculations have not taken into account radiation losses due to impurities since the model for their production, e.g. during neutral injection, is not yet sufficiently clarified. On the other hand, with the assumed Co injection the particle trajectories and the outward shift of the magnetic axis

in high-beta equilibria cause the energy deposition of the neutrals to be displaced to the plasma interior, which should partially compensate the radiation losses in the centre.

2. Particle Trajectory Calculations with the Freya Code

In order to obtain energy deposition in the centre of the plasma for neutral injection heating, an injection system with 160 kV was assumed in keeping with the opacity $n \cdot a$, 60% of the neutrals having an energy of 160 keV, 20% of them 80 keV, and 20% 53 keV (deuterium). The necessary injection angle with respect to the normal to the plasma surface was determined with the Freya code (Monte Carlo method) in conjunction with the vessel and coil concepts (for experimental data see Tabel 1) and the corresponding ripple values ($\pm$ 4% at the plasma boundary). The ripple losses for $\geqslant 20^{\circ}$ Co injection are accordingly below 5%, while the corresponding counter injection leads to losses of up to 20%. As more oblique angles would require a considerable increase in the outlay of the experiment and at the same time, higher beam energies for deposition in the centre, pure Co injection was taken as a basis /1/. Concerning the energy deposition of the injected neutrals we found nearly the same deposition profiles in the Whist code and in the Freya code (see Fig. 1).

Table 1

Zephyr data of Jan. 1979 with compression ratio 1.5

	before compression	after compression
R [m]	1.89	1.26
a [m]	0.57	0.47
A	3.3	2.7
B_{tor} [T]	6.48	9.72
J_{tor} [MA]	2.0	3.3
$q_{current}$	2.6	2.4

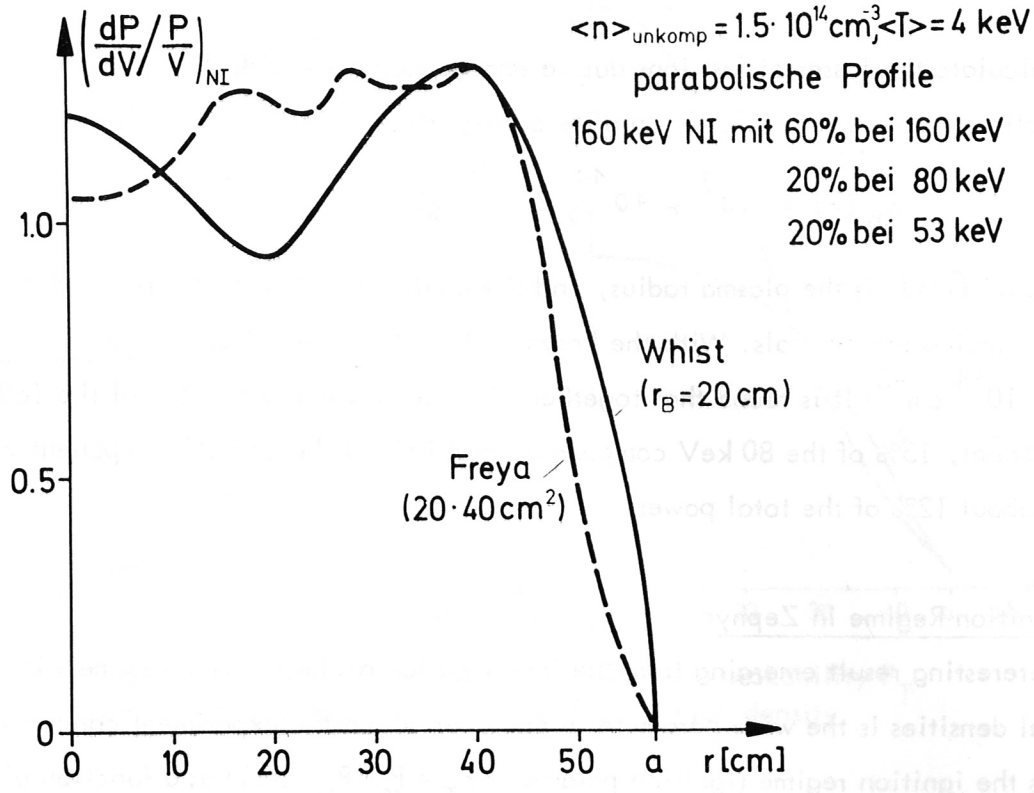

Fig. 1 Local energy deposition with neutral injection according to Whist /3/ and Freya codes /4/, normalized to the mean beam power (without impurities, charge exchange and ripple losses)

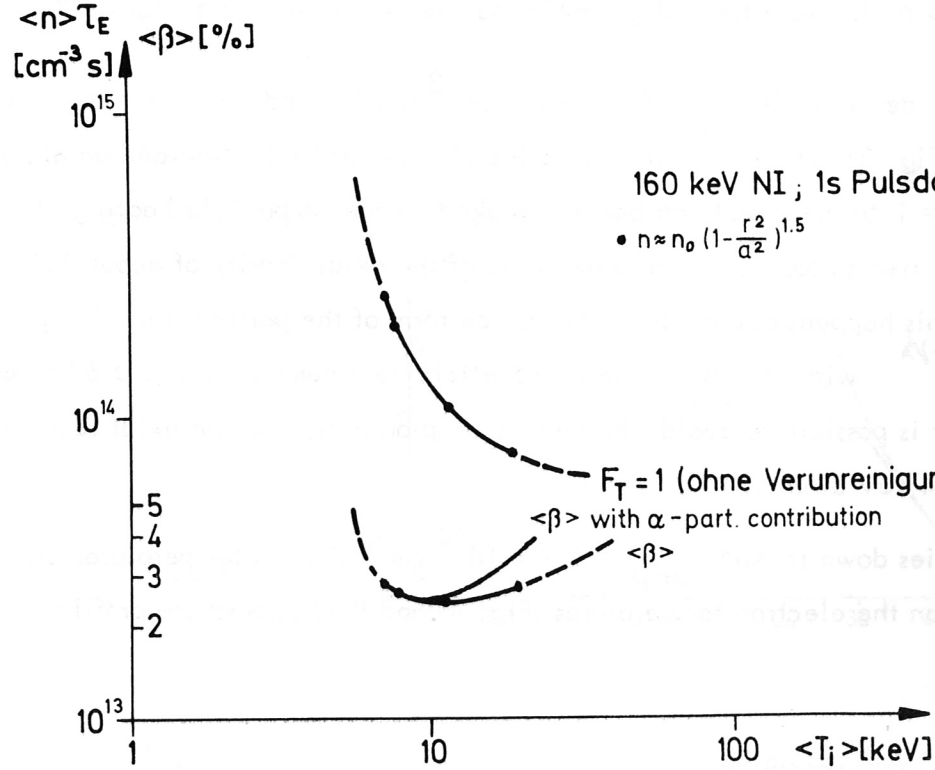

Fig. 2 Ignition regime in Zephyr experiment as a function of $\langle n\rangle\tau_E$, $\langle\beta\rangle$ and $\langle T_i\rangle$ (solid curves).

To calculate the losses of fast ions due to charge exchange with the plasma neutrals, the following neutral gas density profile during gas puffing was assumed:

$$n_n(r) = 10^7 + 10^{11}\, e^{-(a-r)/3} \quad [cm^{-3}]$$

where a [cm] is the plasma radius, and the neutral gas density on axis is determined by recombination neutrals. With the Freya code (20° Co injection; $\langle n_e \rangle_{precomp} = 1.5 \times 10^{14}\ cm^{-3}$) it is found that together with the ripple losses 8.5% of the 160 keV component, 15% of the 80 keV component, and 19% of the 53 keV component are lost, i.e. about 12% of the total power.

3. Ignition Regime in Zephyr

An interesting result emerging from the investigation of the ignition regime with various initial densities is the wide parameter range over which the experiment can work. Figure 2 shows the ignition regime (ignition parameter $F_T = P_\alpha / P_{loss} = 1$) as a function of T_i and $\langle n \rangle \tau_E \sim \langle n \rangle^2 a^2$ which is a very good criterion for ignition. $\langle n \rangle$ is the area-averaged density and τ_E the energy confinement time ($\frac{dW}{dt} = P_{heat} - \frac{W}{\tau_E}$). In all calculations a mixture ratio 50 : 50 of deuterium to tritium was assumed and the neutral heating power is between 14 and 16 MW. The ß values are in the region of $\langle ß \rangle_{tot} \approx 2.5\%$ and, accordingly, $ß_{pol} \approx 1.23 \approx A/2$, while the collisionality parameter varies by a factor of 20.

At the maximum density $\langle n \rangle_{comp} = 4.5 \times 10^{14}\ cm^{-3}$ the ion and electron temperatures are equal (see Fig. 3). The temperature profiles after neutral injection and adiabatic compression (k = 1.5) are broad and become peaked by the α particle heating. Part of the temperature rise on axis is due to a decrease of the axial density of about 20% after compression. This happens according to the source term of the particle refuelling $n = n_b\, e^{-(a-r)/\lambda}$ with $\lambda = 8$ cm within a particle confinement time $\lesssim 0.65$ s. By increasing λ it is possible to avoid the density drop on axis, and the axial temperature rises to about 14 keV after 300 ms.

At lower densities down to $\langle n \rangle_{comp} = 1.7 \times 10^{14}\ cm^{-3}$ the ion temperatures are very much higher than the electron temperatures (Fig. 4) and the temperature profiles are already

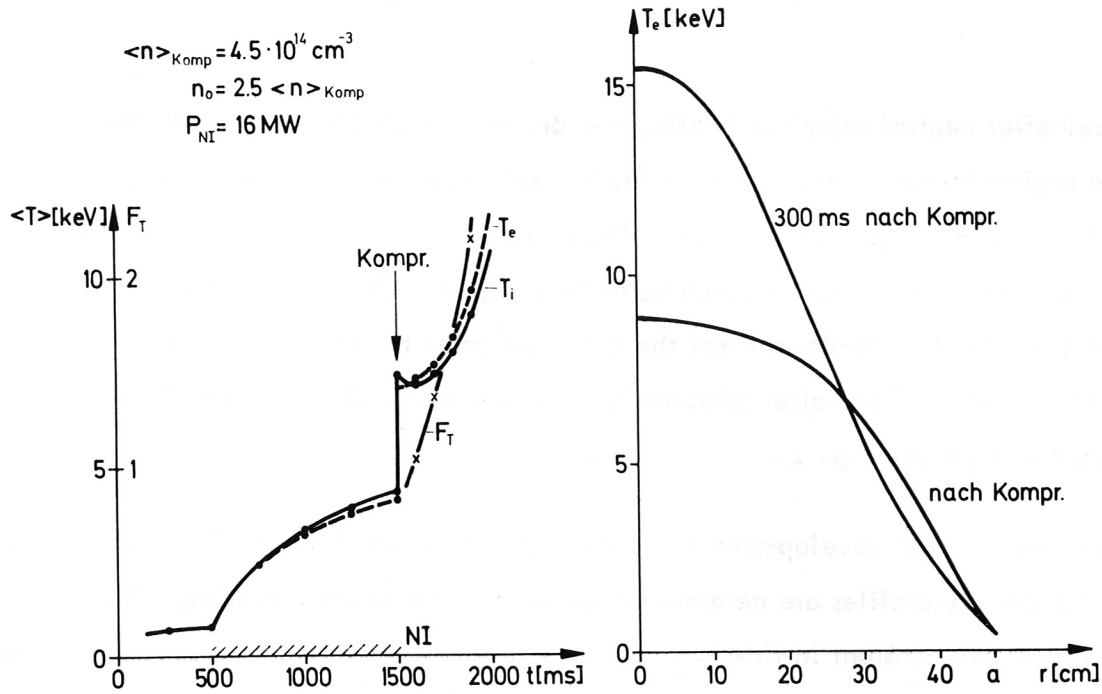

Fig. 3 Time development of temperature and ignition probability F_T and radial electron temperature profiles at high density

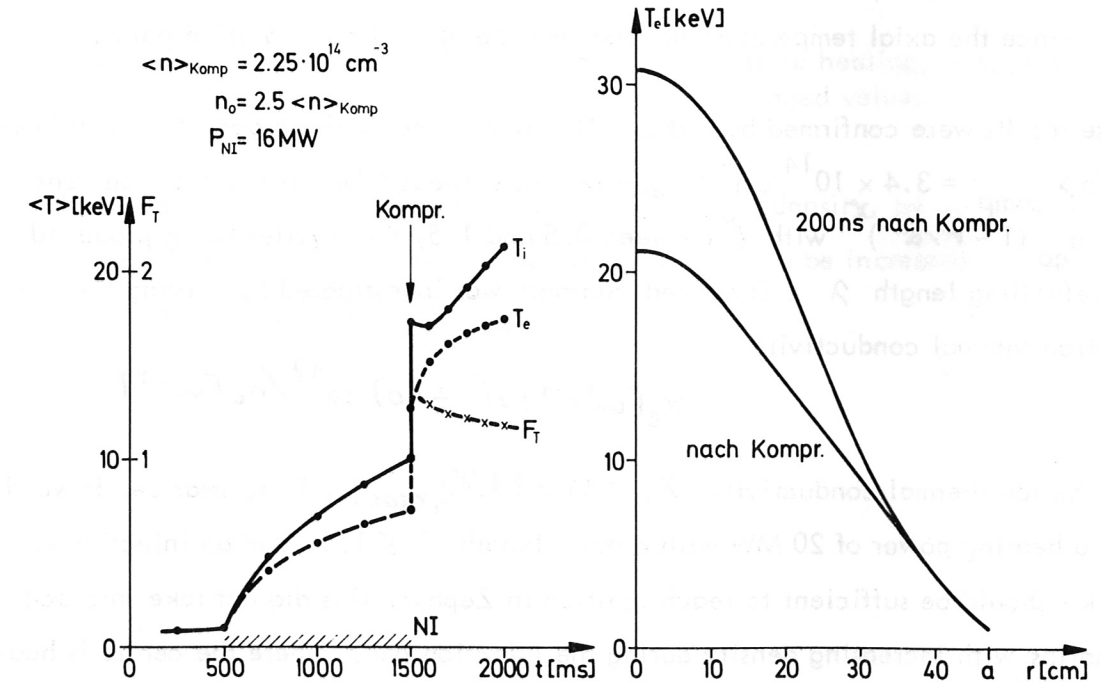

Fig. 4 Time development of temperature and ignition probability F_T and radial electron temperature profiles at low density

peaked after neutral injection heating and are favourable for ignition. In this hot ion mode regime thermal stabilization is facilitated since the axial temperatures very quickly reach the stable upper burning point. The ignition probability F_T therefore also decreases again shortly after adiabatic compression (see Fig. 4). On the other hand, owing to the finite particle slowing-down times the contribution of the fast D^+ ions before compression and of the α particles after compression to ß is already 35%, and stability problems may be encountered (see Fig. 2).

As regards the time development of the density and temperature profiles it should be noted that the density profiles are determined solely by the particle refuelling. The temperature profiles remain constant in time during the neutral injection phase since the α particle heating power is much smaller than P_{NI}. It is only towards the end of the injection phase that the contribution of the α particle heating grows to over 2 MW in the centre of the plasma and becomes almost comparable with the neutral particle heating. After compression the peaking of the T profiles is determined by the α particle heating and hence by the given density profile ($P_\alpha \sim n^2$). As an example Fig. 5 shows the development of the axial values (normalized to the area-averaged values) after compression for a flat density profile. After about one energy confinement time (600 ms) the temperature and α heating profiles flatten again since the axial temperature has reached the upper stable ignition point.

These results were confirmed by further 1D calculations for the proposed standard density of $\langle n \rangle_{comp} = 3.4 \times 10^{14}$ cm^{-3}. Ignition was achieved for various electron density profiles $n_e = n_{eo} (1 - r^2/a^2)^{\gamma}$ with γ between 0.5 and 1.5, the profiles being produced by varying the refuelling length λ. Enhanced transport was investigated by varying the empirical electron thermal conductivity

$$\chi_e [cm^2 s^{-1}] = (5 \div 10)\, 10^{17} / n_e [cm^{-3}]$$

and the ion thermal conductivity $\chi_i = (1 \div 3)\, \chi_{i,neocl}$. To summarize, it was found that a heating power of 20 MW with a pulse length of $\lesssim 1.5$ s and an injection system of 160 kV should be sufficient to reach ignition in Zephyr. This did not take into account scenarios with increasing density during the injection phase where the centre is heated

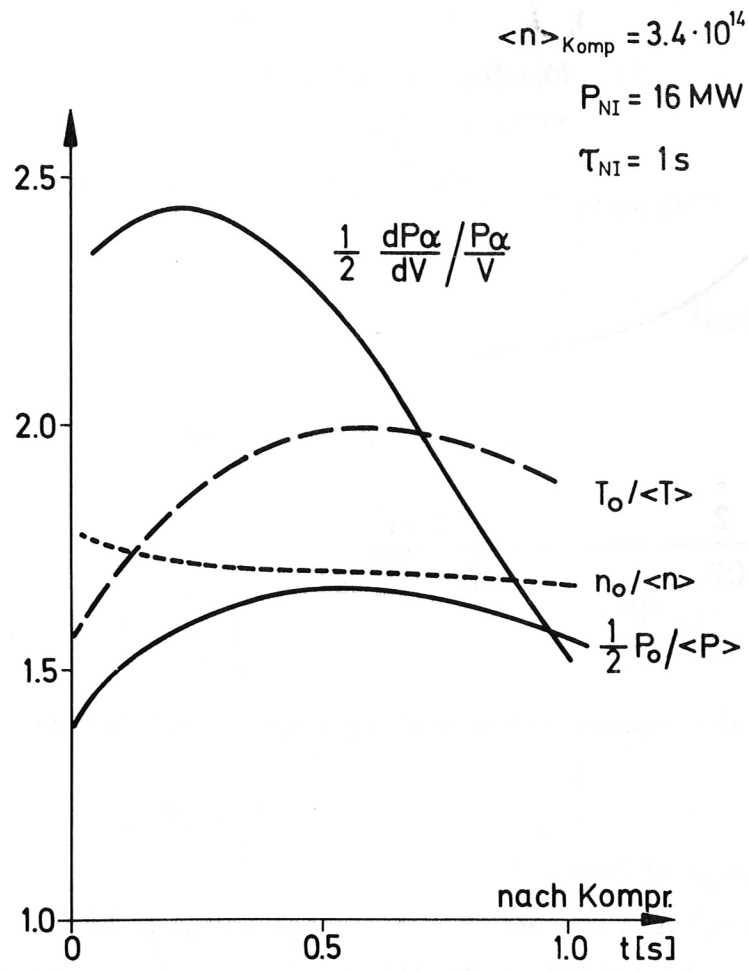

Fig. 5 Time development of the axial values of ∝ particle heating, temperature, density and pressure (normalized to the area-averaged values)

first by the better penetrating neutrals and then, with rising density, by ∝ particles. To achieve equal plasma parameters, the heating power has to be increased strongly for brief heating pulses according to Fig. 6.

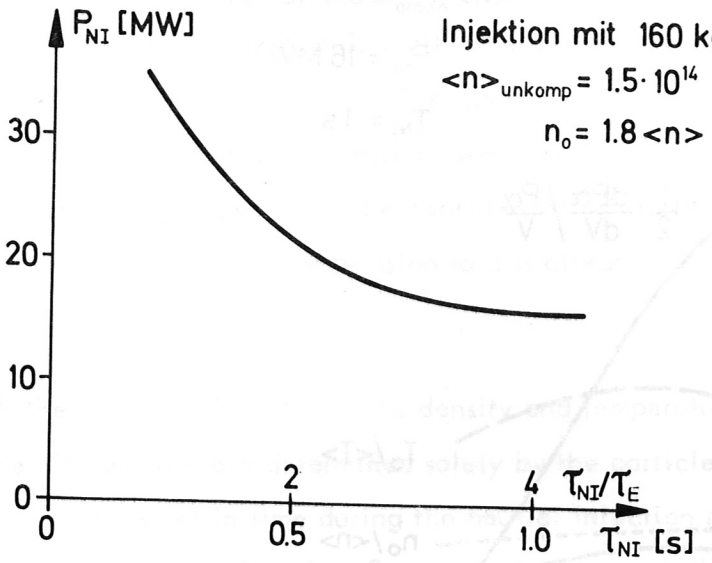

Fig. 6 Dependence of heating power with neutral injection on the injection time

4. Variation of Injection Energy of Neutrals

As neutral particle technology has so far been developed to an energy of 120 keV (TFTR), heating was also investigated with 120 kV and 80 kV injectors in addition to the 160 kV system. In Fig. 7 the depositions for two plasma density profiles and the various injector systems are compared. The more central deposition for the "flat"-density profile is obtained from the 15% smaller line integral $\int ndl$, compared with that for the peaked profile. The simulations show for scenarios which lead to ignition parameters F_T between 0.6 and > 1 after compression that the heat power has to be raised according to

$$P_{NI} \sim \frac{1}{\sqrt{u_{NI}}}$$

(injection time τ_{NI} = 1s). Charge exchange losses (see Sec. 2) and possible increase of the impurity concentration due to the greatly enhanced number of injected neutrals at low energies require, however, higher heating powers, and so a dependence

$$P_{NI} \sim \frac{1}{u_{NI}^{\alpha}}$$

with α in the region of 1 seems plausible.

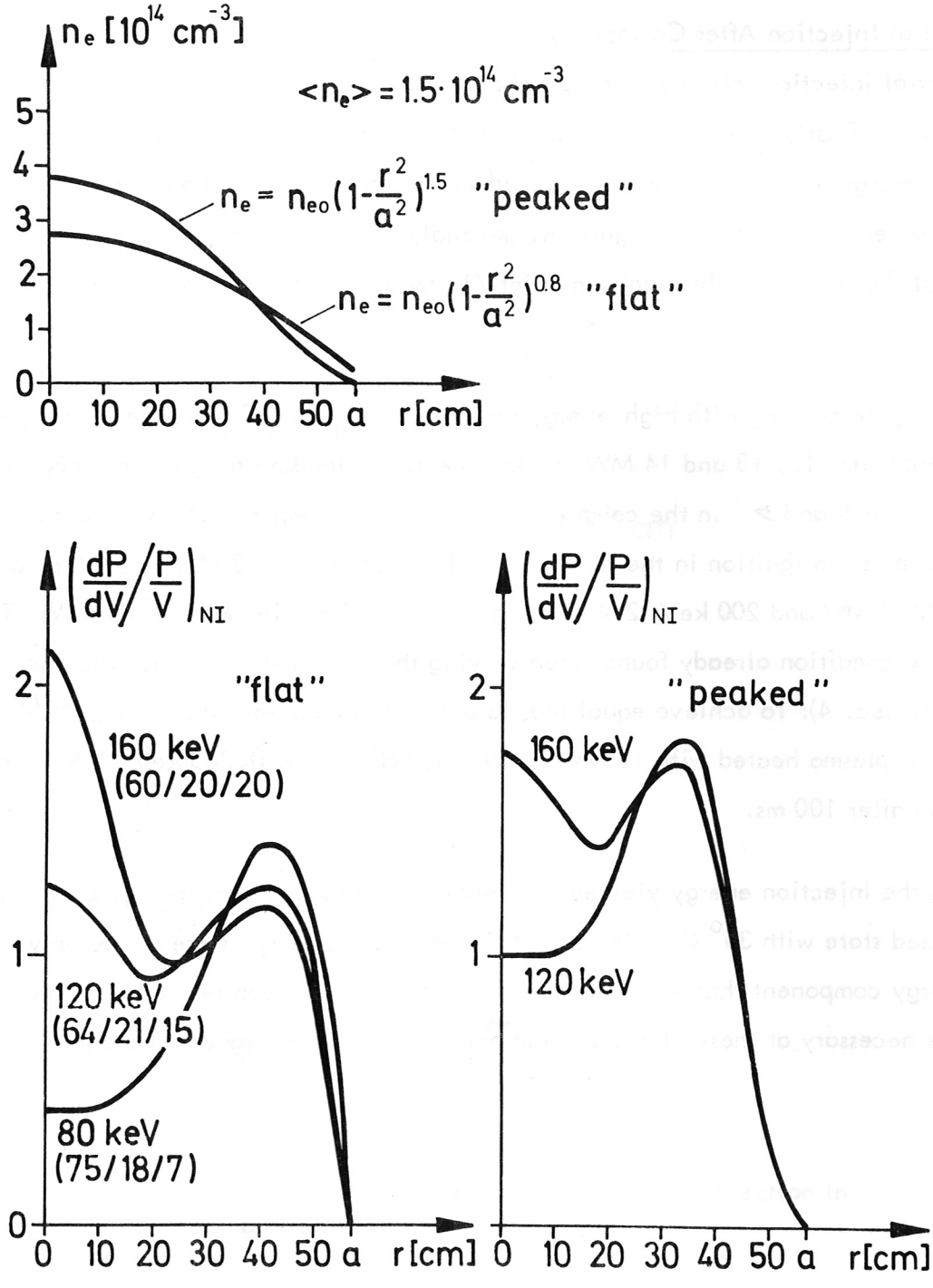

Fig. 7 Local energy deposition profiles with neutral injection in the uncompressed state. In parentheses, the powers of the components with full, half and one-third energy.

5. Neutral Injection After Compression

The neutral injection into the compressed plasma is investigated in the following for two reasons. Firstly, the plasma energy after adiabatic compression, W_o, may be lower than the marginal ignition energy W_m, and so an additional heating power $P_H \geq \frac{W_m - W_o}{\tau_E}$ would be necessary to achieve ignition. Secondly, the plasma might be stabilized in the region of the lower unstable ignition point /1/ by means of a controlled weak additional heating.

To investigate heating with high-energy neutrals ($U_{NI} \geq 200$ keV) the initial plasma was heated with 12, 13 and 14 MW 160 keV neutrals, leading to ignition probabilities $F_T = 0.65$, 0.9 and > 1 in the compressed state (without impurities). By injection of neutrals after compression ignition in the plasma initially heated with 13 MW took place after 300 ms (300 keV; 2 MW and 200 keV; 2.45 MW) and after 450 ms (160 keV; 2.75 MW). This again yields the condition already found when varying the injection energy for the uncompressed state (see Sec. 4): To achieve equal plasma data, it is necessary that $P_{NI} \sim 1/\sqrt{U_{NI}}$ For the initial plasma heated with 12 MW ignition is achieved with 300 keV, 3 MW neutral injection after 100 ms.

Varying the injection energy yielded the deposition profiles shown in Fig. 8 for the compressed state with 35° Co injection at the plasma boundary. Here it was only the full energy component that was considered in keeping with negative ion technology, which becomes necessary at these high injection energies due to its higher efficiency.

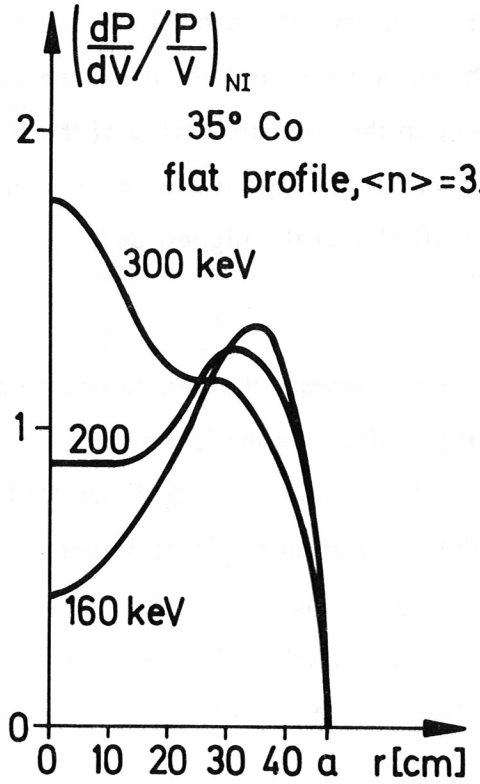

Fig. 8 Local energy deposition profiles with neutral injection in the compressed state

6. Active Burn Control of Nearly Ignited Plasma by Controlled Neutral Injection

For feedback stabilization of the plasma energy at a value slightly below ignition by modulating the neutral injection heating power the time behaviour of the neutron flux ϕ_n is suitable for providing the input to the feedback loop. ϕ_n is proportional to the α - particle heating power $P_\alpha \sim \int n^2 T_i^2 \, dv$ ($T_i < 20$ keV) and, besides being measurable with greater precision, is more sensitive to the energy balance than T_i. The control circuit has to be faster than the time of energy increase at the ignition point ($\tau = W/\frac{dW}{dt} \sim \sigma(\tau_E)$), i.e. a response time of about 200 ms is necessary. The control power should be about 1/10 of P_α ($Q = \frac{\text{fusion power}}{\text{external heating power}} \gtrsim 50$) and may assume only three values: 0, 1/2 and 1 of the maximum power. Then, depending on the time derivative of the flux ϕ_n, the control power will be set to 1, 1/2 and 0 respectively. It should be mentioned that P_α at the marginal ignition energy is between 10 MW at the highest density (4.5×10^{14} cm^{-3}) and 16 MW at the lowest density (2×10^{14} cm^{-3}).

The time behaviour of the α-particle heating power, the plasma energy and the ignition parameter for feedback stabilized, nearly ignited plasma is shown in Fig. 9. The global F_T is somewhat smaller than 0.9, whereas within a radius of $r \lesssim 20$ cm $\approx a/2.5$ the plasma has ignited ($F_T > 1$). Towards the end of the simulation the ignition parameter goes above 0.9 and control is no longer possible since energy cannot be withdrawn from the plasma. This is in contrast to burn stabilization by, for instance, adiabatic compression and decompression. In all simulations with $F_T > 0.9$ the plasma ignites within one energy confinement time.

The values on axis normalized to the averaged values given in Fig. 10 indicate the time development of the profiles. Temperature and α-particle heating profiles become peaked without external heating and stay constant during the neutral injection heating phase owing to the broader heating profiles (see fig. 8). This demonstrates the possibility of neutral injection for tailoring the temperature profile. The peaking of the T-profile during simulation corresponds to an e-folding time of 30 s for $T_o / \langle T \rangle$.

In the calculation shown internal sawtooth disruptions have not been taken into account, so that the q-value on axis drops to 0.6. Using the Kadomtsev Model to describe the internal

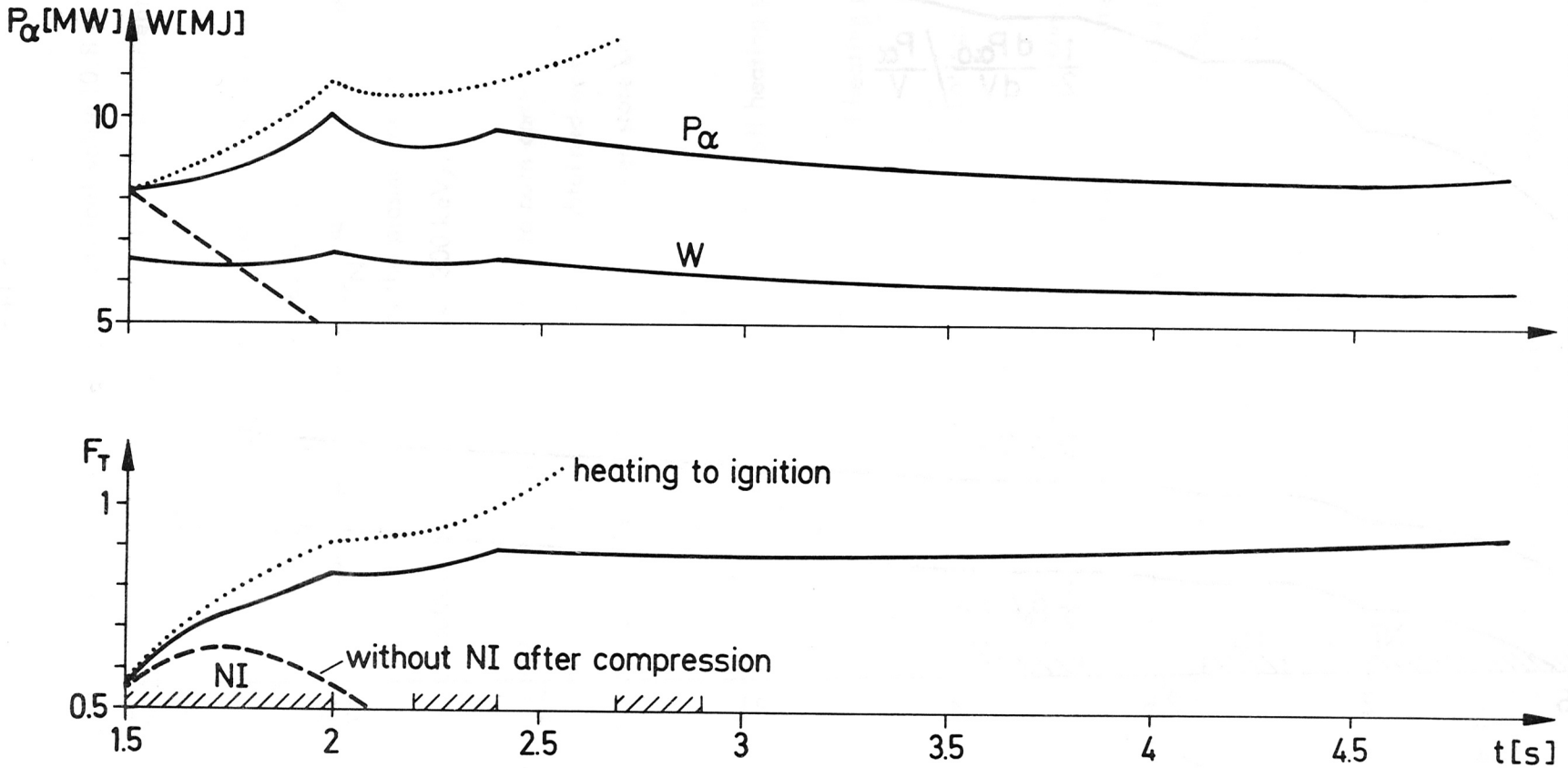

Fig. 9 Time behaviour of α - particle heating power P_α, plasma energy W and ignition parameter F_T in the compressed plasma with active burn control by neutral injection ($\langle n_e \rangle = 3.\delta \times 10^{14}$ cm^{-3}).

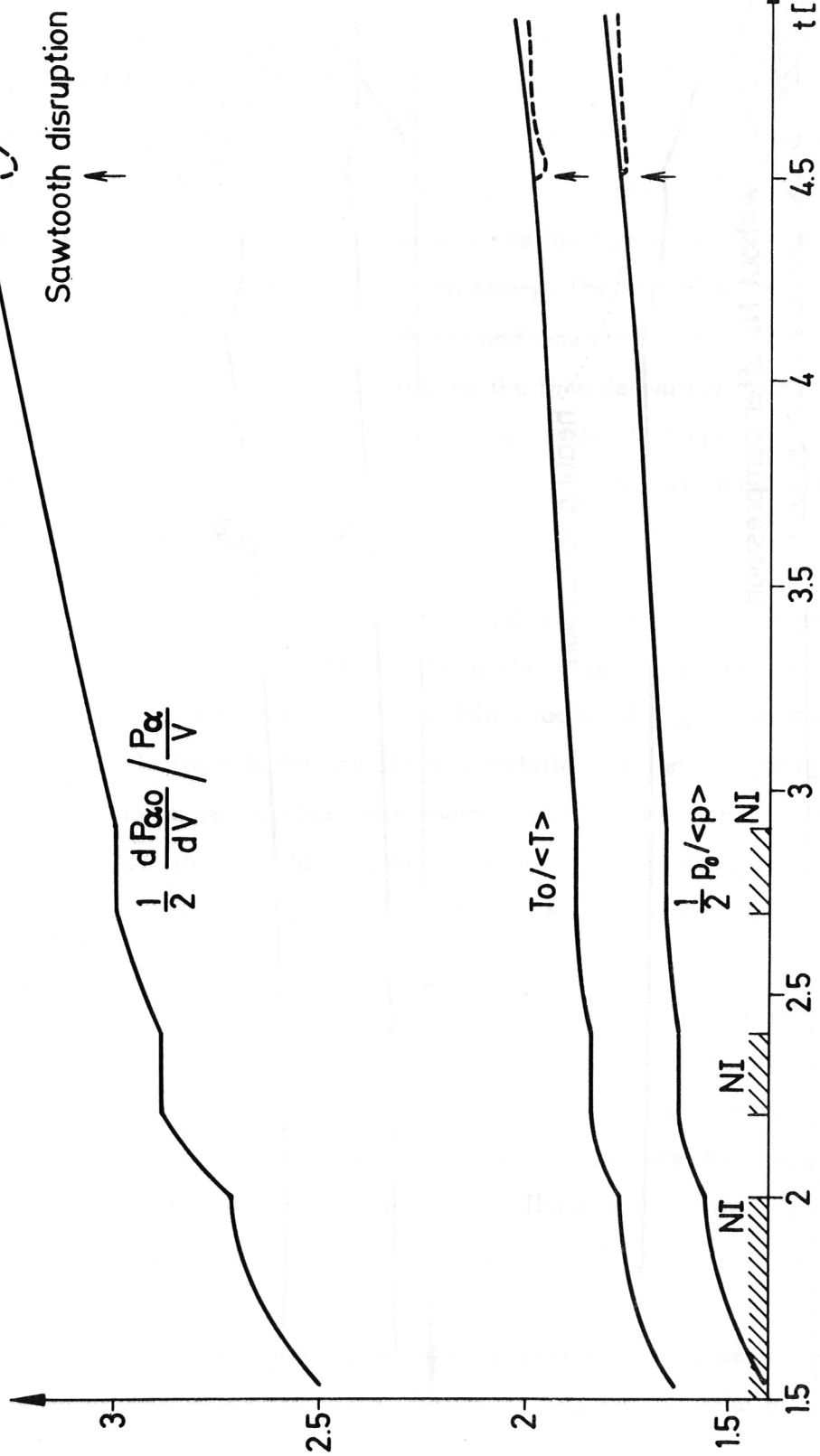

Fig. 10 Time behaviour of the local values on axis (normalized to the averaged values) of α - particle heating power $\frac{dP_\alpha}{dV}\Big/\frac{P_\alpha}{V}$, temperature $(T_e + T_i)_o / (\langle T_e\rangle + \langle T_i\rangle)$ and pressure $p_o/\langle p\rangle$. The density profile was kept constant by refuelling: $n = n_o(1 - r^2/a^2)^{0.75}$; $\langle n\rangle = 3.8 \times 10^{14}$ cm^{-3}. The influence of an internal sawtooth disruption is shown at 4.5 s (dashed curve).

disruptions /5,6/ whenever q_o becomes smaller than a critical value (0.8 to 0.95) one obtains periodical flattening of the temperature, density and toroidal current density near the axis with a period of about 300 ms. Correspondingly, the α - particle heating is reduced and this helps to stabilize the ignited plasma centre. The influence of an internal disruption ($q_{crit} = 0.8$) is shown in Fig. 10 at 4.5 sec. A rule is that without internal disruptions one should have an edge auxiliary heating ($U_{NI} \approx 200$ keV), as the α - particles heat mainly the centre. But with internal disruptions the plasma centre needs heating and demands for higher neutral beam energy ($U_{NI} \approx 300$ keV).

The results of the previous 1-d calculations with respect to burn control are summarized in the following. In the non-driven state ignition ($F_T > 1$) is obtained when $\dot{\phi}_n \sim \dot{P}_\alpha \geq 0$ exists for longer than one energy confinement time. In the driven state one has to achieve the following scheme derived from the power balance:

$$\dot{\phi}_n / \phi_n < -\delta/\tau_E \qquad \text{full heating power,}$$

$$-\delta/\tau_E < \dot{\phi}_n / \phi_n < \delta/\tau_E \qquad \text{half heating power,}$$

$$\delta/\tau_E < \dot{\phi}_n / \phi_n \qquad \text{no heating.}$$

The value of $\delta << 1$ and the control power depend sensitively on the difference between the plasma energy and the marginal ignition energy. A plasma near the lower unstable burning point is hard to stabilize. Global stabilization at $F_T \approx 0.9$, corresponding to $Q \approx 50$, requires that $\delta \approx 0.05$, i.e. deviations of P_α have to be kept below 4%, and of T_i below 2%. If $F_T < 0.9$ or $Q < 50$, higher δ and temperature deviations are permitted. This parameter range is being investigated at present.

The author wishes to acknowledge the valuable discussions with K. Lackner and to thank D. Pohl and J.E. Faulkner for their assistance with the computations.

References

/1/ Compact Ignition Experiment (Sept. 1978), Internal Status Report IPP

/2/ Compact Ignition Experiment Project Proposal (Jan. 1979) IPP

/3/ W.A. Houlberg, R.W. Conn, Proc. Topical Meeting on "Improved Methods of Analysis of Nuclear Systems" (1977)

/4/ G.G. Lister, D.E. Post, R.J. Goldston, Proc. Third Symp. on Heating in Toroidal Plasmas, Varenna (1976), p. 303

/5/ W.A. Houlberg, J.T. Hogan, IEEE Conf. on Plasma Science, Montreal, Canada (1979), 5B7

/6/ B.B.Kadomtsev, Sov. J. Plasma Phys. 1, 389 (1975)